Supplementary Information

Oxidation and adduct formation of xenobiotics in a microfluidic electrochemical cell with boron doped diamond electrodes and an integrated passive gradient rotation mixer

Floris T.G. van den Brink,[a] Tina Wigger,[bc] Liwei Ma,[a] Mathieu Odijk,[a*] Wouter Olthuis,[a] Uwe Karst[bc] and Albert van den Berg[a]

[a] BIOS – Lab on a Chip group, MESA+ Institute for Nanotechnology and MIRA institute for Biomedical Technology and Technical Medicine, University of Twente, Enschede, The Netherlands

[b] Institute of Inorganic and Analytical Chemistry, Westfälische Wilhelms-Universität Münster, Münster, Germany

[c] NRW Graduate School of Chemistry, Westfälische Wilhelms-Universität Münster, Germany

* E-mail: m.odijk@utwente.nl

Table S1: Settings and operating conditions of the Time-of-Flight mass spectrometer.

	1-OHP MV	**+GSH**	**+LGA**	**+Hb**
Mass range (m/z)	100-600	100-1200	300-3000	300-3000
Nebulizer gas pressure (bar)	0.8	0.8	1.8	1.8
Dry gas flow rate (L/min)	4	4	8	8
Dry gas heater temperature (°C)	180	180	190	180
Capillary voltage (V)	4000	4500	4000	4000
Endplate offset voltage (V)	-500	-500	-300	-300
Capillary exit voltage (V)	120	150	150	180
Skimmer 1 voltage (V)	40	50	50	60
Skimmer 2 voltage (V)	24.6	24	22.5	22
Hexapole 1 voltage (V)	26.7	25	25	23
Hexapole 2 voltage (V)	21	20	20	21
Hexapole RF voltage (Vpp)	60	400	450	500
Lens transfer time (µs)	49	52	60	70
Pre-pulse storage time	1	15	30	30
Lens 1 storage voltage (V)	40	40	40	40
Lens 1 extraction voltage (V)	21.1	20	20	21.1
Lens 2 voltage (V)	7.4	7.4	7.4	7.4
Lens 3 voltage (V)	22	22	22	22
Lens 4 voltage (V)	0.3	0.3	0.3	0.3
Lens 5 voltage (V)	-27.5	-27.5	-27.5	-27.5

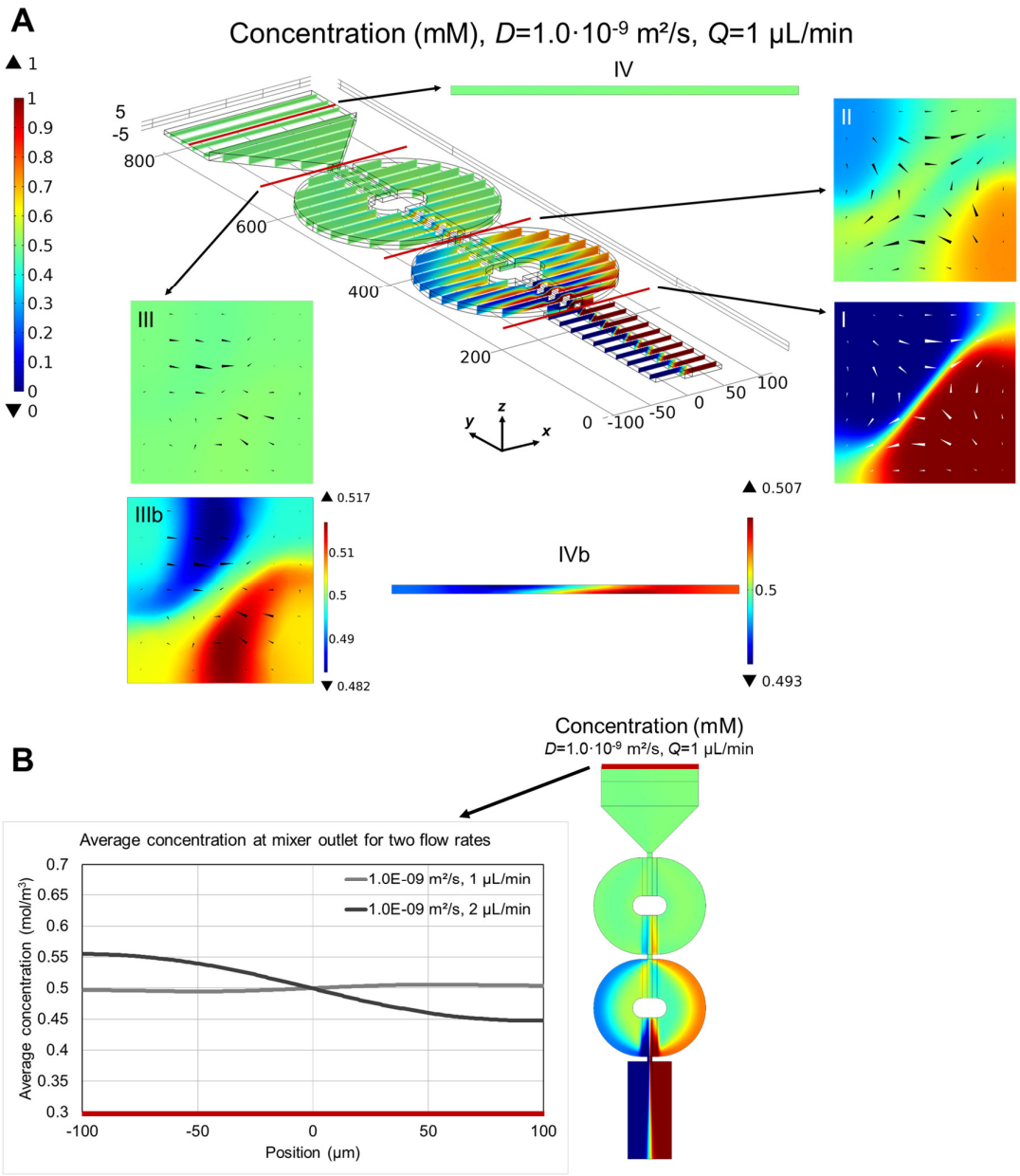

Figure S2: Numerical simulation results of the gradient rotation mixer (obtained using COMSOL v5.1). A: 3D plot of the mixer (including spatial dimensions in µm and coordinate system) containing slices with concentration profiles across the mixer, showing the gradient to be stretched out inside the two mixing chambers. *Insets*: cross-sectional view of the concentration profiles in the three 10 x 10 µm² 'necks'. Note that in IIIb and IVb the color scale is adjusted to allow visualization of the profiles. The arrows represent *x* and *z* components of the flow velocity field. For this simulation, a mixing efficiency of 99% is calculated using eqn 4 in the main text. B: Concentration distribution at the center of the mixer. Along the red line, the concentration is averaged over the channel depth and plotted as a function of position for diffusion coefficient D=1.0·10^{-09} m² s^{-1} and total flow rates of 1 and 2 µL min^{-1}. In these traces and plots, a different concentration profile can be observed compared to Fig. 3 in the main text: the alternative combination of parameters (higher D, lower Q) results in reduced rotation of the concentration gradient as a result of reduced advection and more rapid diffusion.

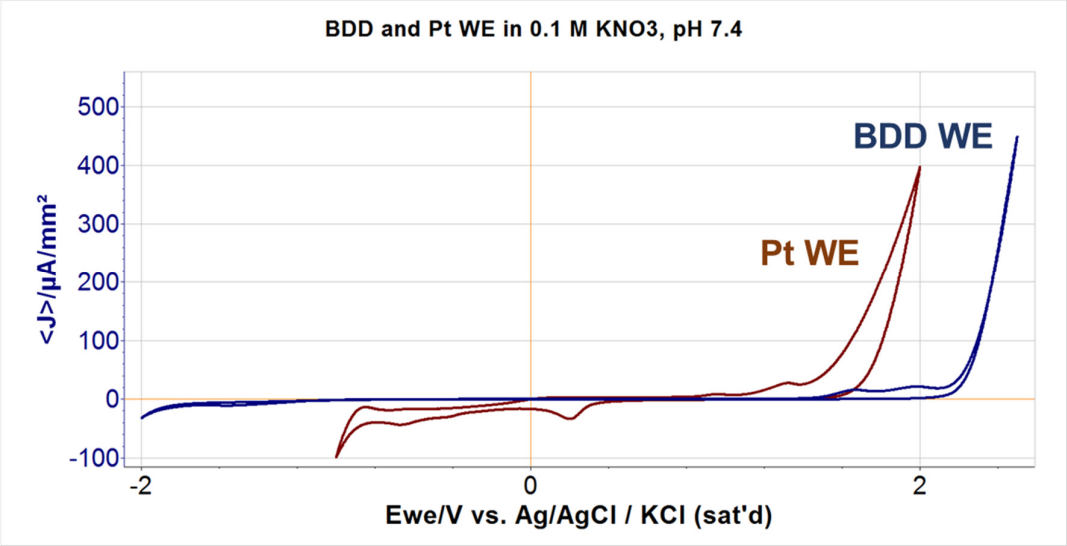

Figure S3: The potential window of the BDD electrodes was determined off-chip in a 0.1 M KNO_3/10 mM phosphate buffer solution (pH 7.4). A micro-structured BDD WE (4.8 mm^2) was compared to a platinum WE (2.5 mm^2) in a macroscopic (regular) electrochemical cell with a platinum CE and a KCl saturated Ag/AgCl RE. Cyclic voltammograms recorded at 100 mV s^{-1} with both WEs show that the BDD electrode has a mainly featureless CV over a potential range of -2 to 2.2 V, providing a potential window of 4.2 V, while this is only 2.6 V for platinum due to the onset of water electrolysis. Adapted with permission from reference 44. Copyright 2016 American Chemical Society.